ISTITUTO NAZIONALE DI FISICA NUCLEARE

INFN/BE - 68/8
15 Giugno 1968

R. Giacomich, L. Granata, M. Lagonegro and G. Pauli:

PRELIMINARY EXPERIMENTAL TESTS ON Si^{28} CONCERNING THE MEASUREMENT OF THE RATIO $\sigma(n,n'\gamma)/\sigma(n,p)$

103

PRELIMINARY EXPERIMENTAL TESTS ON Si^{28}
CONCERNING THE MEASUREMENT OF THE RATIO
$\sigma(n,n'\gamma)/\sigma(n,p)$

R. Giacomich, L. Granata, M. Lagonegro and G. Pauli

Istituto di Fisica dell'Università - Trieste
Istituto Nazionale di Fisica Nucleare - Sottosezione di Trieste

104

1. - INTRODUCTION

This paper reports the preliminary results of an experiment, which is now in progress, concerning the determination of the ratio between the cross-section of the $(n,n'\gamma)$ reaction and the cross-section of the (n,p) reaction for 14 MeV neutrons and nuclei of light and medium atomic weight, for which the (n,p) reaction is followed by a beta decay leading to an excited state of the original nucleus.

The preliminary measurements have been performed with a sample of silicium and particular attention has been given to the de-excitation gamma ray of 1778.9 keV emitted in the transition of the Si^{28} nucleus from the first excited state to the ground state [1]. The gamma rays were detected by means of NaI(Tl) crystals.

2. - DETERMINATION OF THE RATIO $\sigma(n,n'\gamma)/\sigma(n,p)$

When a nucleus ${}_zX^A$ is exposed to a beam of 14 MeV neutrons, it can partecipate either to the inelastic scattering reaction

$$(1) \qquad {}_zX^A + n \rightarrow n' + \left[{}_zX^A\right]^* ,$$

where the original nucleus is normally left in an excited state from which it decays with the emission of gamma radiation, or to the (n,p) reaction

$$(2) \qquad {}_zX^A + n \rightarrow p + {}_{z-1}Y^A ,$$

where the final nucleus can be beta -emitter, in which case it transforms itself into the original nucleus according to the decay scheme

$$(3) \qquad {}_{z-1}Y^A \rightarrow \beta^- + \left[{}_zX^A\right]^* .$$

We restrict ourselves to consider only those nuclei ${}_zX^A$ which, when resulting from the radioactive decay (3), are always found in their first excited state.

Then, let us have a beam of 14 MeV neutrons impinging upon a sample which containes the ${}_{z}X^{A}$ isotope and let us measure both the energy spectrum of the gamma rays emitted in the inelastic scattering reaction (1) (prompt gamma rays) and the energy spectrum of the gamma rays emitted in the radioactive decay(3) (delayed gamma rays).

The prompt spectrum will show a number of peaks due to the ${}_{z}X^{A}$ nucleus which correspond to the allowed transitions of this nucleus. On the other hand, the delayed spectrum will contain only one peak due to the ${}_{z}X^{A}$ nucleus produced in the reaction (3): precisely the peak corresponding to the transition of this nucleus from the first excited level to the ground level.

Now, if N_1 is the number of prompt gamma rays counted in τ_1 seconds and associated with the transition of the ${}_{z}X^{A}$ nucleus from the first excited level to the foundamental level, one has

$$N_1 = \Phi \frac{\mathcal{N}}{A} \rho V \sigma(n,n'\gamma_1) \tau_1 \epsilon(\gamma_1) \tag{4}$$

where:

Φ = incident neutron flux ($cm^{-2} sec^{-1}$) ,

$\mathcal{N}$ = Avogadro's number,

A = mass number of the target nucleus ,

ρ = density of the sample (g/cm^3) ,

V = volume of that part of the sample which effectively intracts with the neutron beam (cm^3) ,

$\sigma(n,n'\gamma_1)$ = cross-section for the production of the de-excitation gamma ray (γ_1) corresponding to the transition of the ${}_{z}X^{A}$ nucleus from the first excited level to the ground level in the inelastic scattering of 14 MeV neutrons, (barns) ,

$\epsilon(\gamma_1)$ = photo-peak efficiency of the NaI(Tl) crystal in the energy range of the gamma-ray γ_1.

At the end of the time interval τ_1, the sample will contain a number n of radionuclides $_{z-1}Y^A$ given by

$$(5) \qquad n = \Phi \frac{\mathcal{N}}{A} \rho \, V \, \sigma(n,p) \, \frac{1-e^{-\lambda\tau_1}}{\lambda}$$

where: $\sigma(n,p)$ = cross-section for the reaction (n,p) ,

λ = disintegration constant of the radio-nuclide $_{z-1}Y^A$ (sec^{-1}).

If now one measures the gamma activity of the sample for τ_2 seconds, the number N_1' of the (delayed) gamma rays associated with the transition of the $_zX^A$ nucleus from the first excited level to the ground level is expressed by the equation

$$(6) \qquad N_1' = \int_0^{\tau_2} \lambda n e^{-\lambda t} \, dt = \Phi \frac{\mathcal{N}}{A} \rho \, V \, \sigma(n,p) \, \frac{(1-e^{-\lambda\tau_1})(1-e^{-\lambda\tau_2})}{\lambda} \times$$

$$\times \, \epsilon(\gamma_1) \, .$$

From eq.s (4) and (6) one derives

$$(7) \qquad \frac{\sigma(n,n'\gamma_1)}{\sigma(n,p)} = \frac{N_1}{N_1'} \, \frac{1}{\lambda\tau_1} \, (1-e^{-\lambda\tau_1}) \, (1-e^{-\lambda\tau_2}) \, .$$

3. - EXPERIMENTAL APPARATUS

The measurements have been performed using the 14 MeV neutrons produced by bombarding a tritium target with the deuterons accelerated by means of the 600 keV Cockroft-Walton of the Istituto di Fisica di Trieste.

In Fig. 1 a block diagram of the experimental apparatus is shown.

The α-particle detector was a NE 810 scintillator crystal coupled with a 56 AVP photomultiplier. The γ-rays were detected by means of a NaI(Tl) crystal coupled with a 6292 Dumont photomultiplier.

An electronic timer (Fig. 2 and Fig. 3) performes the following cycle of operations on the "magnet control unit" (m.c.u.) and on the "multichannel control unit" (M.c.u.) during three successive time intervals τ_1, τ_2 and τ_3.

a) Time interval τ_1. During this interval, the length of which can be varied from 1' to 30', the m.c.u. is operated in such a way as to maintain the deuteron beam on the tritium target, meanwhile the M.c.u. is operated so as to open the first subgroup of 100 channels of a 200 channel-analyzer. Under these conditions, using a fast-slow coincidence circuit, one can measure the energy spectrum of the gamma rays which are in coincidence, within 100 nsec, with the α-particles associated with the neutrons which interact with the sample. This spectrum will contain the gamma peaks due to the (n,n' γ) reactions. In the experiment, the length of the interval τ_1, was taken equal to $\sigma \times T_{1/2}$, where $T_{1/2}$ is the half life of the radiosotope produced in the (n,p) reaction.

b) Time interval τ_2. During this interval, which can be varied from 1' to 20', the m.c.u. is operated in order to move the deuteron beam away from the tritium target, meanwhile the M.c.u. opens the second subgroup of 100 channels of the multichannel analyzer and excludes the fast-slow coincidence circuit. In these conditions, one measures the energy spectrum of the γ-activity of the sample, which is due principally to the (n,p) reactions,of Si^{28} with the 14 MeV neutrons,which have taken place during the irradiation time τ_1.

c) Time interval τ_3. During this interval, which is taken equal to $\tau_1 - \tau_2$, the deuteron beam is still moved away from the tritium target and the multichannel analyzer is excluded. Under these conditions, no neutron is produced and the radioactivity induced in the sample during τ_1 has time long enough to decay almost completely.

At the end of the time interval τ_3, the cycle of operations a), b) and c) is repeated.

4. - EXPERIMENTAL RESULTS

The preliminary measurements described in this report concern the determination of the ratio $\sigma(n,n'\gamma_1)/\sigma(n,p)$ for the Si^{28} nucleus with reference to the γ_1-ray emitted in the transition of the Si^{28} from the first excited level to the ground level.

The scattering sample used was in the form of a right cylinder and consisted of five elements 4 cm long and 6.3 cm in diameter. Each sample element was made of powder of natural Silicium (92.18% of Si^{28}, 4.71% of Si^{29}, 3.12% of Si^{30}) contained in a thin-walled perspex cylinder.

The measurements can be divided in the following three groups:

1. measurements of the prompt gamma ray spectra in the range from about 100 keV to about 6200 keV;
2. measurements of the angular distribution of the γ_1-ray;
3. cyclic measurements of prompt and delayed gamma spectra.

4.1 Measurements of the prompt gamma ray spectrum in the range from 100 keV to 6200 keV.

These measurements have been performed using a 2" × 2" NaI(Tl) crystal in the range from 100 keV to 3200 keV (Fig. 4) and a 3" × 3" NaI(Tl) crystal from 1500 keV to 6200 keV (Fig. 5). A background spectrum is shown in Fig.6.

By inspection of the spectra of Fig. 4 and Fig. 5, one can recognize a rather pronounced peak, corresponding to the 1778.9 keV transition of Si^{28}, and a structure which, in spite of the rather low counting statistics and high background, indicates the presence of other γ-rays. These γ-rays can be attributed to different reactions of the 14 MeV neutrons with Si^{28} or with other materials present in the neighborhood of the γ-detector, such as Na^{23} and I^{127} contained in the scintillation crystal itself, Al, Fe, Pb contained in the shields, frames and so on. The position of some of these γ-rays, according with their energy, has been numbered in the Fig. 4, Fig. 5 and Fig.6; the probable reaction and the production cross-section at 90° is indicated in table 1 ([2]).

4.2 Measurements of the angular distribution of the 1778.9 keV gamma-ray(γ_1).

These measurements have been performed with the 2" × 2" NaI (Tl) crystal and using only one of the sample elements described in par. 4.

The experimental data regarding the angular distribution of the 1778.9 keV gamma-ray are shown in Fig.7. ϑ_0 is the angle of observation of the gamma-rays with respect to the direction of the incident neutron beam. $f(\vartheta)$ represents the counting rate normalized to the counting rate at 90°.

4.3 Cyclic measurements of the prompt spectrum and the delayed spectrum.

The spectrum of the prompt gamma-rays and the spectrum of the delayed gamma-rays measured with the 2"×2" NaI(Tl) crystal are shown in Fig. 8 and Fig. 9 respectively.

The number of counts under the 1778.9 keV γ-peak is $N_1 = 543 \pm 66$ in the prompt spectrum and $N_1' = 79 \pm 12$ in the delayed spectrum.

5. - NUMERICAL EVALUATION OF THE $\sigma(n,n'\gamma_1)$

On the basis of Eq. (7) one may write

$$(8) \qquad \int_{\vartheta_1}^{\vartheta_2} \frac{d\sigma(n,n'\gamma_1)}{d\Omega}\, d\Omega = \frac{N}{N_1'} \left[\int_{\vartheta_1}^{\vartheta_2} \frac{d\sigma(n,p)}{d\Omega}\, d\Omega \right] \frac{1.44\, T_{1/2}}{\tau_1} \times$$

$$\times \, (1-e^{-\lambda \tau_1})(1-e^{-\lambda \tau_2})$$

where it is $T_{1/2} = \dfrac{0.693}{\lambda} = 138$ sec.

Assuming for the cross-section $\sigma(n,p)$ the value of 240 mb, as suggested by Cuzzocrea et al. [3], one obtaines for $\vartheta_1 = 50°$ and $\vartheta_2 = 130°$

$$(9) \qquad \int_{\vartheta_1}^{\vartheta_2} \frac{d\sigma(n,p)}{d\Omega}\, d\Omega = 154 \text{ mb}.$$

By inserting this value in (8) and using the values N_1 and N_1' riported in par. 4.3, the left hand side integral of the expression (8) becomes equal to 67 mb.

Now, by putting

$$\frac{d\sigma(n,n'\gamma_1)}{d\Omega} = k\, f(\vartheta) \quad \text{mb/sr}\ , \tag{10}$$

from the expression

$$\int_{\vartheta_1}^{\vartheta_2} \frac{d\sigma(n,n'\gamma_1)}{d\Omega}\, d\Omega \equiv 2\pi \int_{\vartheta_1}^{\vartheta_2} \frac{d\sigma(n,n'\gamma_1)}{d\Omega} \sin\vartheta\, d\vartheta = \tag{11}$$

$$= 2\pi \sum_{i=1}^{5} k\, f(\vartheta_i) \sin\vartheta_i\, \Delta\vartheta_i = 67 \text{ mb}$$

where the values $f(\vartheta_i)$ are those represented in Fig. 7, one can derive the value of the normalization factor k.

The differential cross-section determined in this way is shown in Fig.10. By making the least-squares fit to the data with the function [4]

$$\sigma(\vartheta) = a + b\, P_2\ (\cos\vartheta) + c\, P_4\ (\cos\vartheta) \tag{12}$$

the following expression is found

$$\sigma(\vartheta) = 10.6 + 10.1\, P_2\ (\cos\vartheta) + 2.1\, P_4\ (\cos\vartheta) \quad \text{mb/sr} \tag{13}$$

which gives for the total cross-section for the production of the 1778.9 keV gamma ray from Si^{28} the value

$$\sigma(1778.9 \text{ keV}) = \int_0^{2\pi} 2\pi\, \sigma(\vartheta) \sin\vartheta\, d\vartheta = 133 \pm 40 \text{ mb}\ . \tag{14}$$

The error is determined principally by the rather low counting statistics.

The value (14) agrees with the value of 106±16 mb given by Clarke and Cross [5] for the total inelastic cross-section for the first excited level of Si^{28}.

Many thanks are due to Prof. G. Poiani for having stimulated the present work and for helpful discussion.

The work was accomplished with the technical help of Mr. S. Jasnig and Mr. G. Kidric.

* * *

REFERENCES

(1) E.F. GIBSON, K. BATTLESON and D.K. Mc DANIELS: Phys Rev. 172, 1004 (1968).

(2) F.C. ENGESSER and W.E. THOMPSON: J. Nucl. En. 21, 487 (1967).

(3) P. CUZZOCREA, S. NOTARRIGO, P. PERILLO: Report INFN/BE-67/10 (1967),
Report INFN/BE-67/11 (1967),
Report INFN/BE-67/13 (1967).

(4) D.T. STEWART and P.W. MARTIN: Nucl. Phys. 60, 349 (1964).

(5) R.L. CLARKE and W.G. CROSS: Nucl. Phys. 53, 177 (1964).

* * *

TABLE 1 - Identification of γ-rays appearing in the spectra of Fig. 4, Fig. 5 and Fig. 6.

Spectrum of Figure	γ-peak	E_γ (keV)	Probable reaction	Production cross-section (mb/sr at 90°) (†) (2)
4	1	960	Si^{28} (n,α) Mg^{25} *	4.4 ± 1.5
	2	1240	Si^{29} (n,n') Si^{29} *	-
	3	1300	Al^{27} (n,n') Al^{27} *	2.1 ± 0.7
	4	1790	Si^{28} (n,n') Si^{28} *	46.9 ± 4.7
	5	1920	?	-
	6	2160	Al^{27} (n,n') Al^{27} *	10.8 ± 1.1
			Na^{23} (n,n') Na^{23} *	3.2 ± 1.1
	7	2900	Si^{28} (n,n') Si^{28} *	5.3 ± 0.6
5	1	1780	Si^{28} (n,n') Si^{28} *	46.9 ± 4.7
	2	1950	?	-
	3	2300	Na^{23} (n,n') Na^{23} *	3.2 ± 1.1
	4	2850	Si^{28} (n,n') Si^{28} *	5.3 ± 0.6
	5	3580	?	-
	6	3850	?	-
	7	4420	Si^{28} (n,n') Si^{28} *	1.2 ± 0.4
	8	4970	Si^{28} (n,n') Si^{28} *	3.9 ± 0.8
6	1	1300	Al^{27} (n,n') Al^{27} *	2.1 ± 0.7
	2	1700	Al^{27} (n,n') Al^{27}*	4.3 ± 1.4

(†) The values of this column represent the production cross-section integrated from 90° to 110°.

FIGURE CAPTIONS

Fig. 1 - Schematic diagram of the experimental setup.

Fig. 2 - Block-diagram of the electronic timer.

Fig. 3 - Electronic Timer schematic.

Fig. 4 - Pulse height distribution of γ-rays from Silicon.

Fig. 5 - Pulse height distribution of γ-rays from Silicon.

Fig. 6 - Background spectrum measured with the 2" x 2" NaI(Tl) crystal.

Fig. 7 - Angular distribution of the 1778.9 keV γ-ray from Si^{28}.

Fig. 8 - Pulse height distribution of the prompt γ-rays from silicon.

Fig. 9 - Pulse height distribution of the delayed γ-rays from silicon.

Fig. 10 - Differential cross-section for the 1778.9 keV transition in Si^{28}. The solid curve rappresents the least-squares fit.

* * *

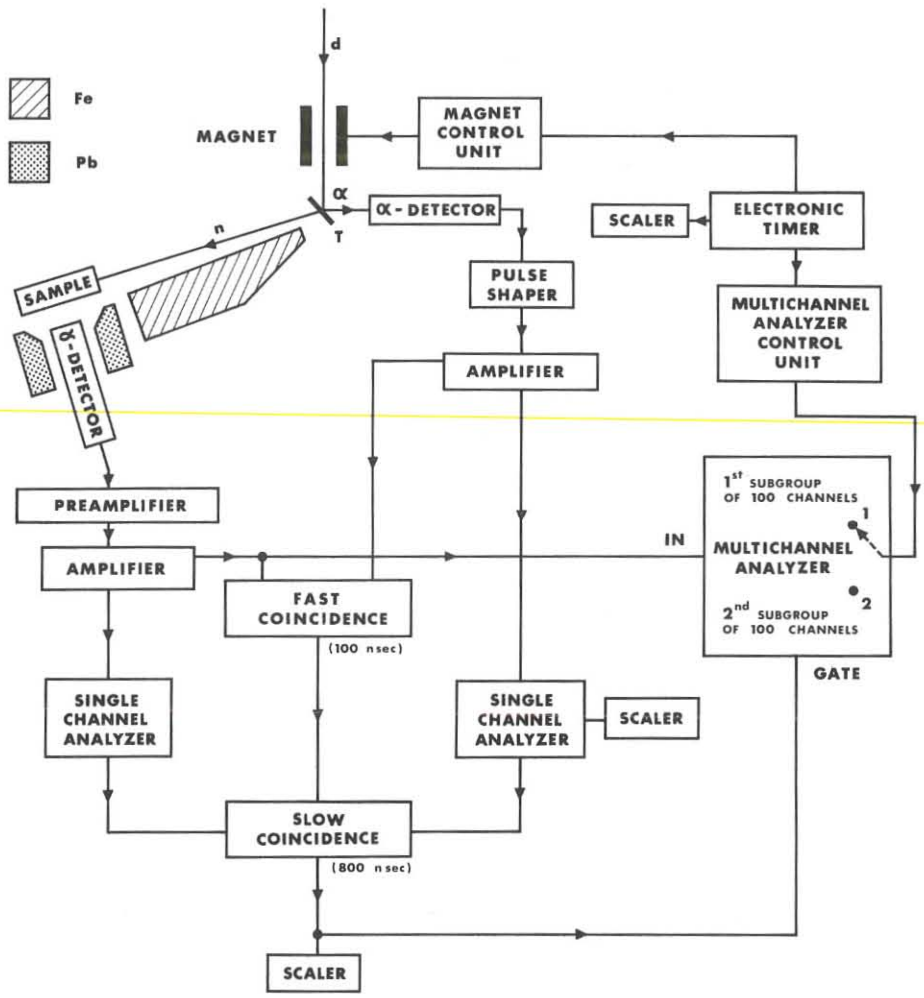

Fe
Pb
d
MAGNET
MAGNET CONTROL UNIT
α
T
α - DETECTOR
n
SAMPLE
α - DETECTOR
SCALER
ELECTRONIC TIMER
PULSE SHAPER
MULTICHANNEL ANALYZER CONTROL UNIT
AMPLIFIER
PREAMPLIFIER
AMPLIFIER
IN
1st SUBGROUP OF 100 CHANNELS
1
MULTICHANNEL ANALYZER
2
2nd SUBGROUP OF 100 CHANNELS
FAST COINCIDENCE
(100 nsec)
GATE
SINGLE CHANNEL ANALYZER
SINGLE CHANNEL ANALYZER
SCALER
SLOW COINCIDENCE
(800 nsec)
SCALER

Fig. 1

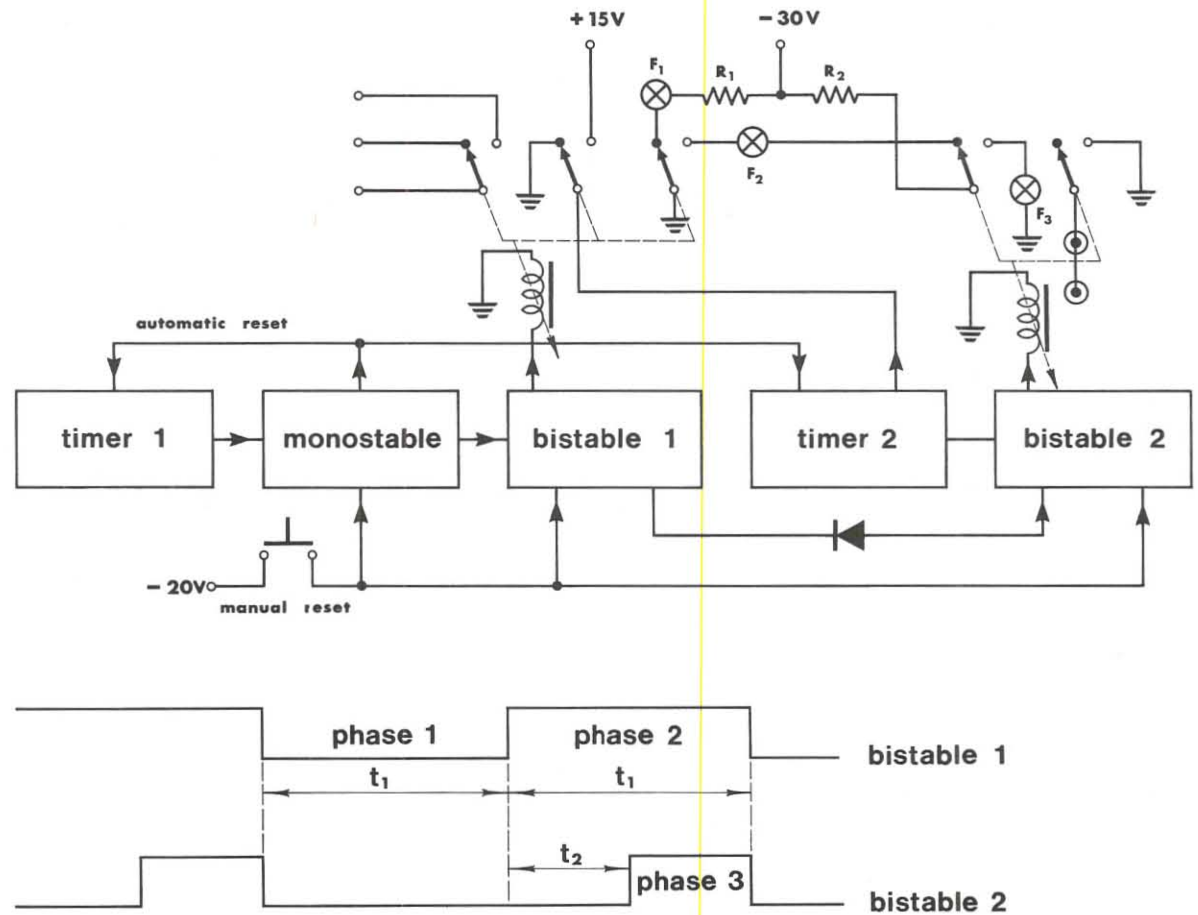
+15V
-30V
F1
R1
R2
F2
F3
automatic reset
timer 1
monostable
bistable 1
timer 2
bistable 2
-20V
manual reset
phase 1
phase 2
phase 3
t1
t1
t2
bistable 1
bistable 2

Fig. 2

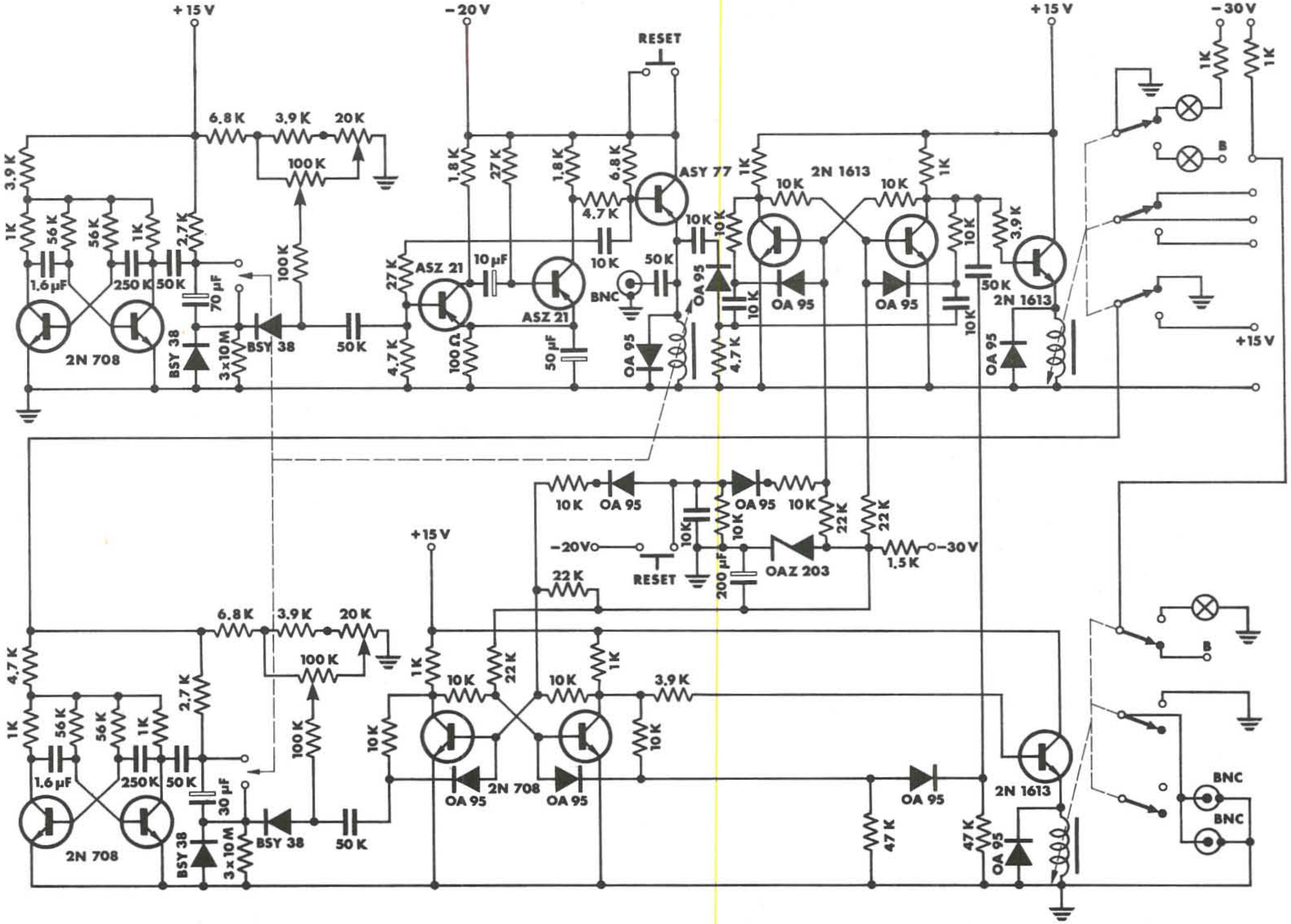
+15 V
−20 V
RESET
+15 V
−30 V
6,8 K
3,9 K
20 K
100 K
3,9 K
1K
56 K
56 K
1K
2,7 K
1,6 µF
250 K
50 K
70 µF
2N 708
BSY 38
3x10M
BSY 38
100 K
50 K
1,8 K
27 K
1,8 K
6,8 K
4,7 K
ASY 77
27 K
ASZ 21
10 µF
ASZ 21
10 K
50 K
BNC
4,7 K
100 Ω
50 µF
OA 95
10 K
1K
10 K
2N 1613
10 K
1K
10 K
3,9 K
OA 95
OA 95
50 K
2N 1613
10 K
OA 95
+15 V
B
10 K
OA 95
OA 95
10 K
22 K
22 K
−20 V
10 K
10 K
RESET
200 µF
OAZ 203
1,5 K
−30 V
22 K
+15 V
6,8 K
3,9 K
20 K
100 K
4,7 K
1K
56 K
56 K
1K
2,7 K
1,6 µF
250 K
50 K
30 µF
2N 708
BSY 38
3x10M
BSY 38
100 K
50 K
1K
10 K
22 K
10 K
1K
3,9 K
10 K
10 K
OA 95
2N 708
OA 95
OA 95
47 K
47 K
OA 95
2N 1613
B
BNC
BNC

Fig. 3

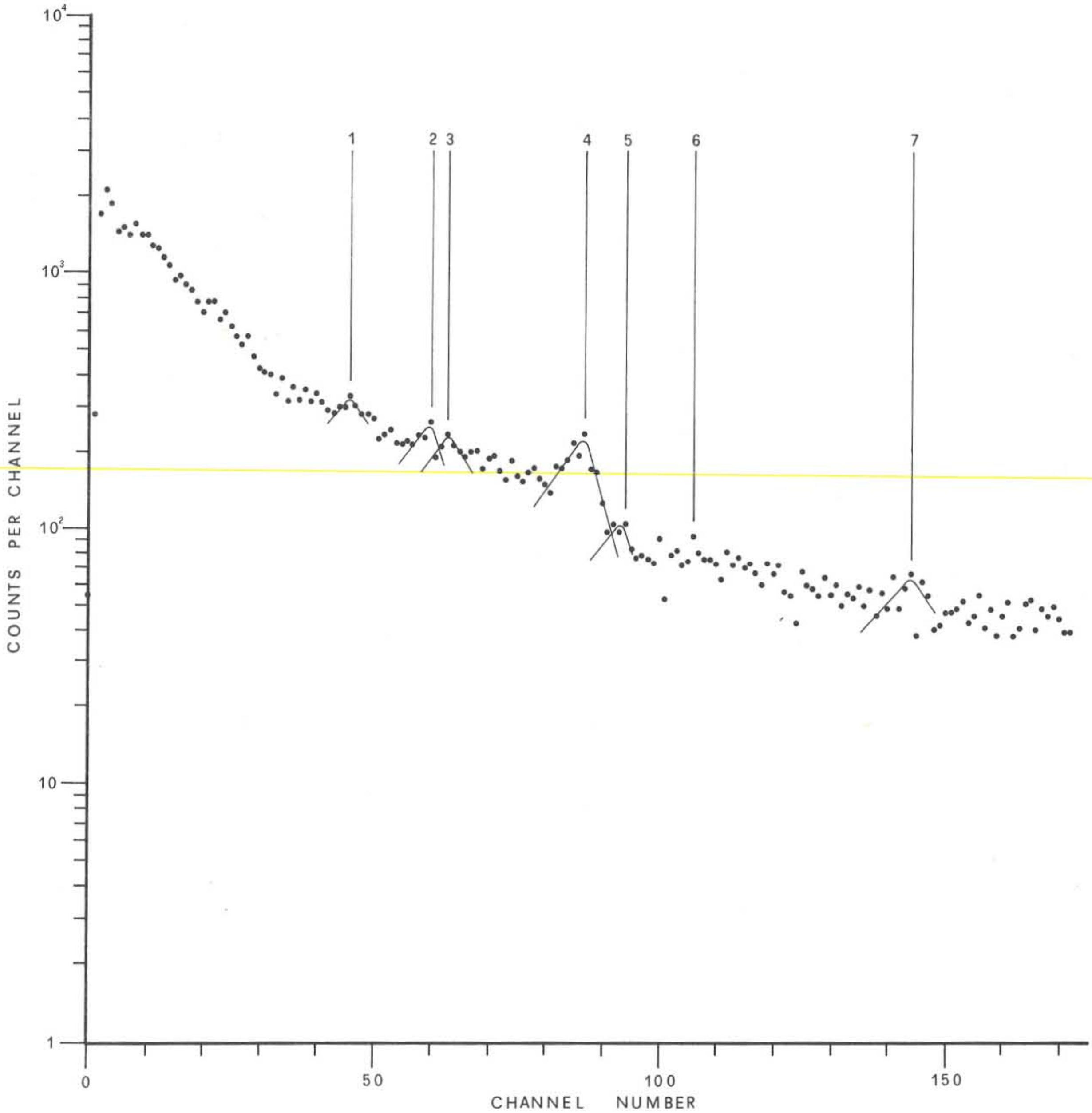

10^4
10^3
10^2
10
1
COUNTS PER CHANNEL
1
2 3
4
5
6
7
0
50
100
150
CHANNEL NUMBER

Fig. 4

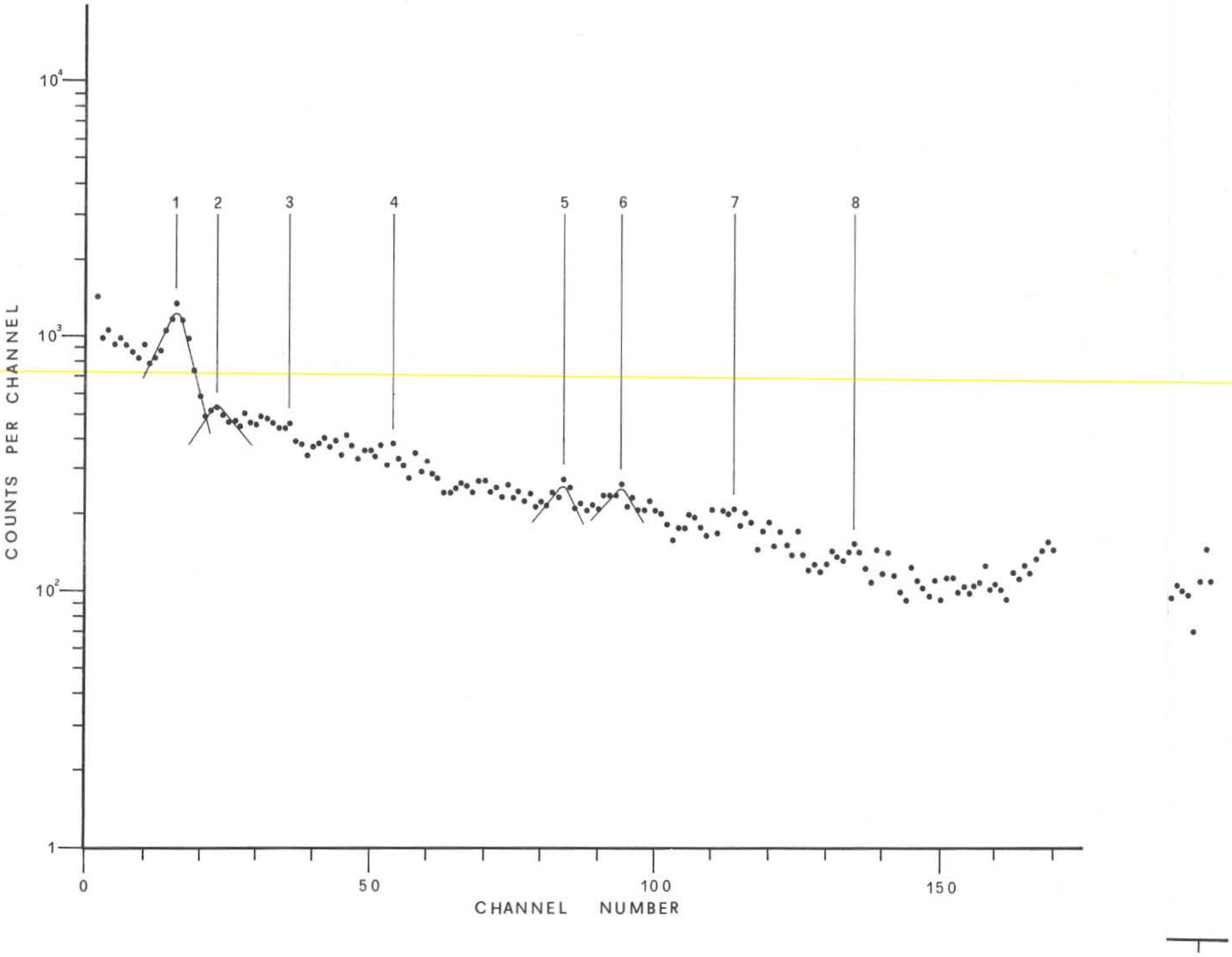
1
2
3
4
5
6
7
8
10^4
10^3
10^2
1
COUNTS PER CHANNEL
0
50
100
150
CHANNEL NUMBER

Fig. 5

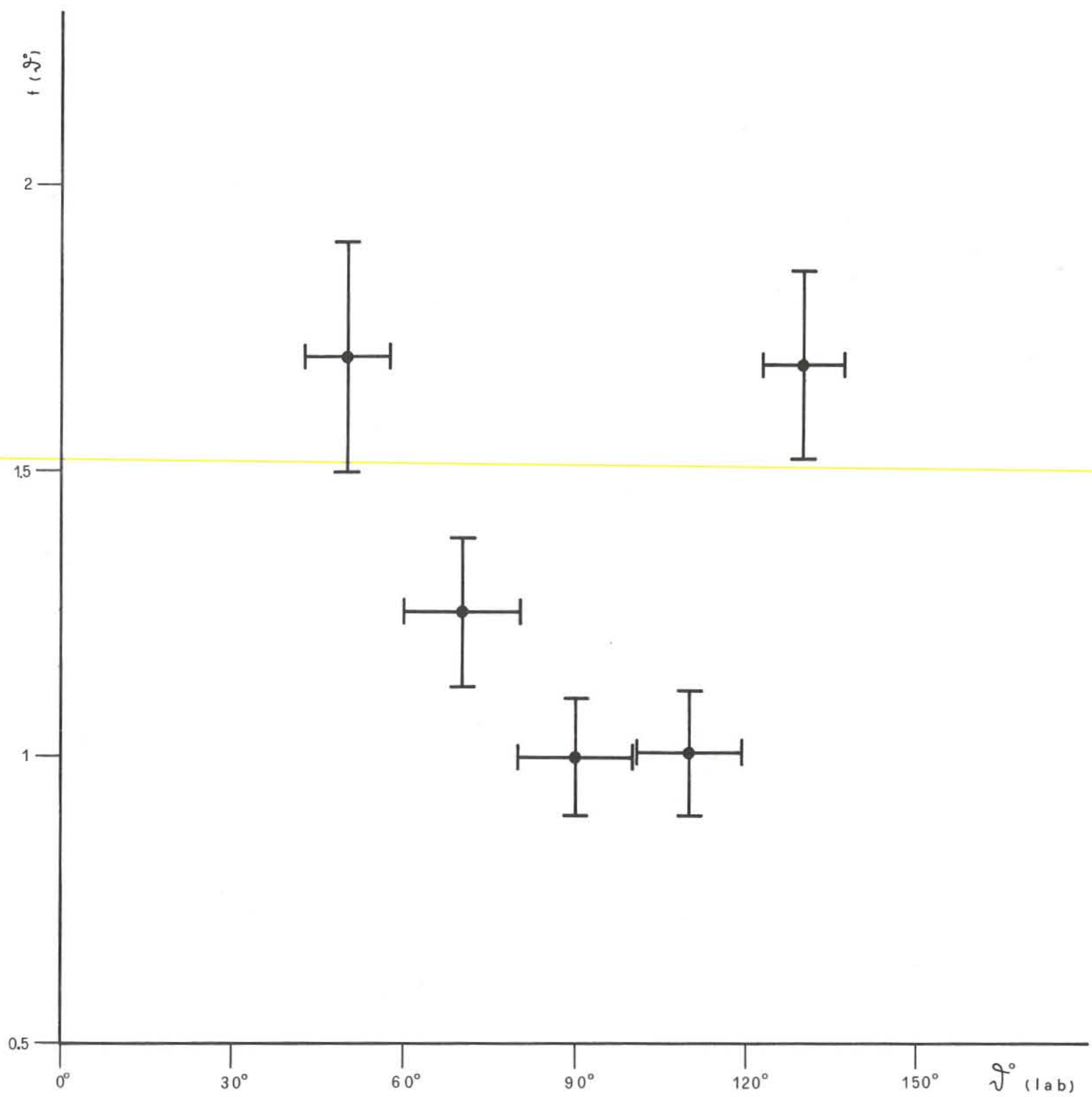

Fig. 7

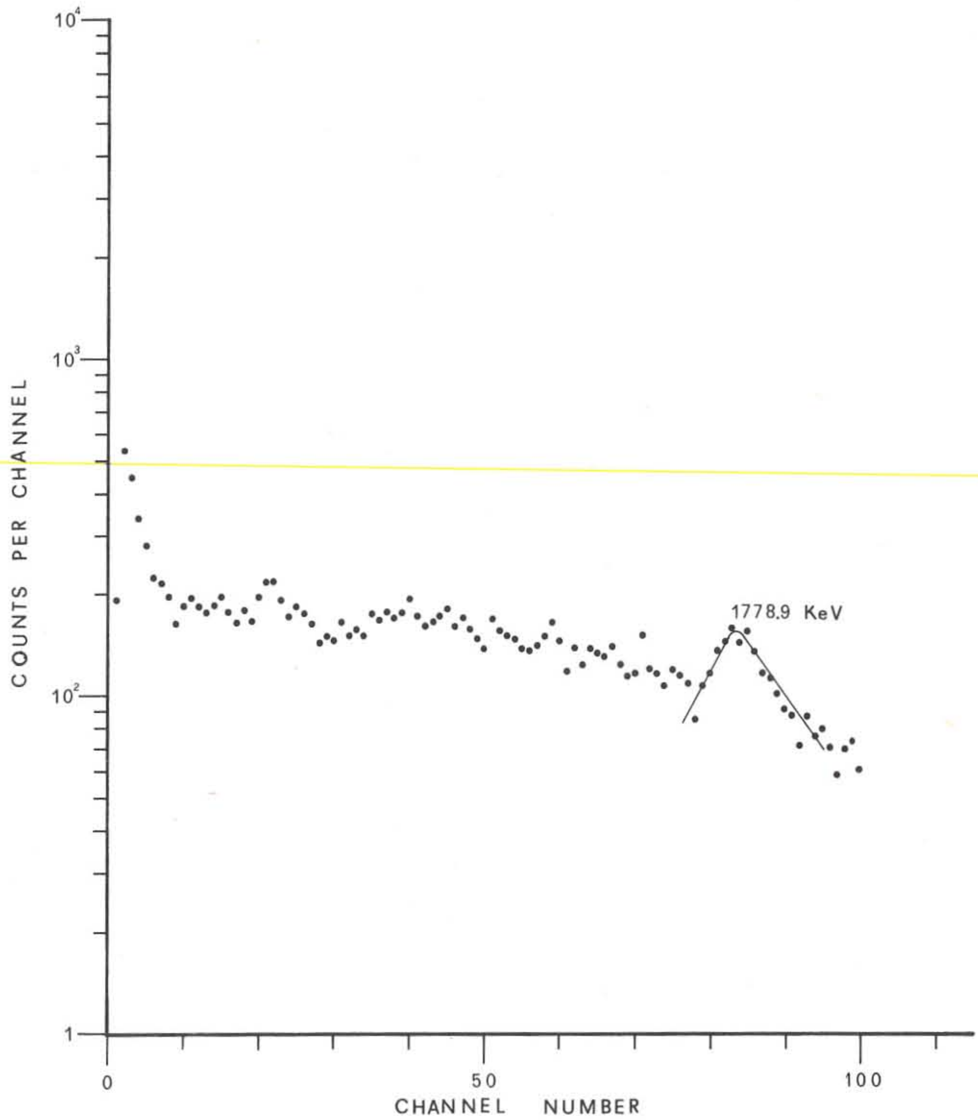

10^4
10^3
10^2
1
COUNTS PER CHANNEL
1778.9 KeV
0
50
100
CHANNEL NUMBER

Fig. 8

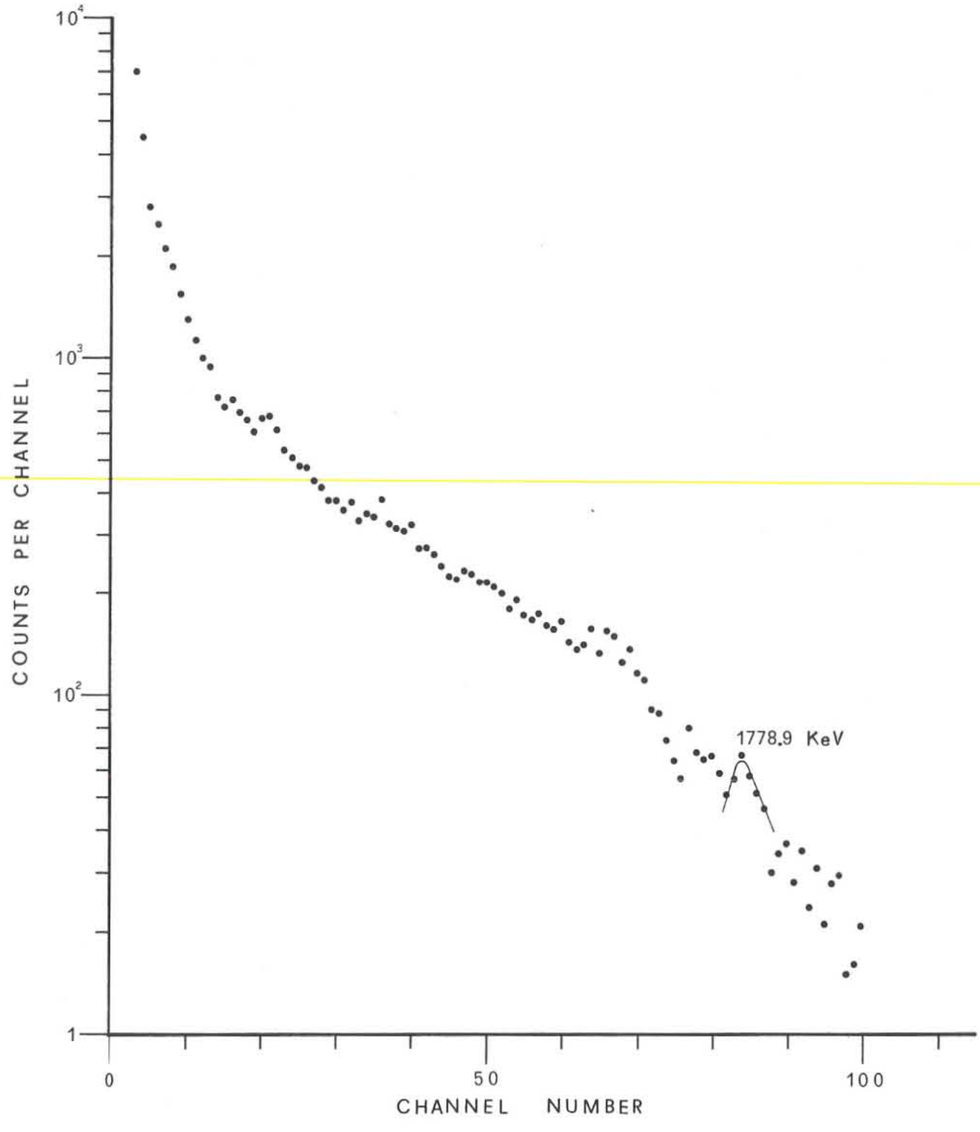

10^4
10^3
10^2
1
COUNTS PER CHANNEL
1778.9 KeV
0
50
100
CHANNEL NUMBER

Fig. 9

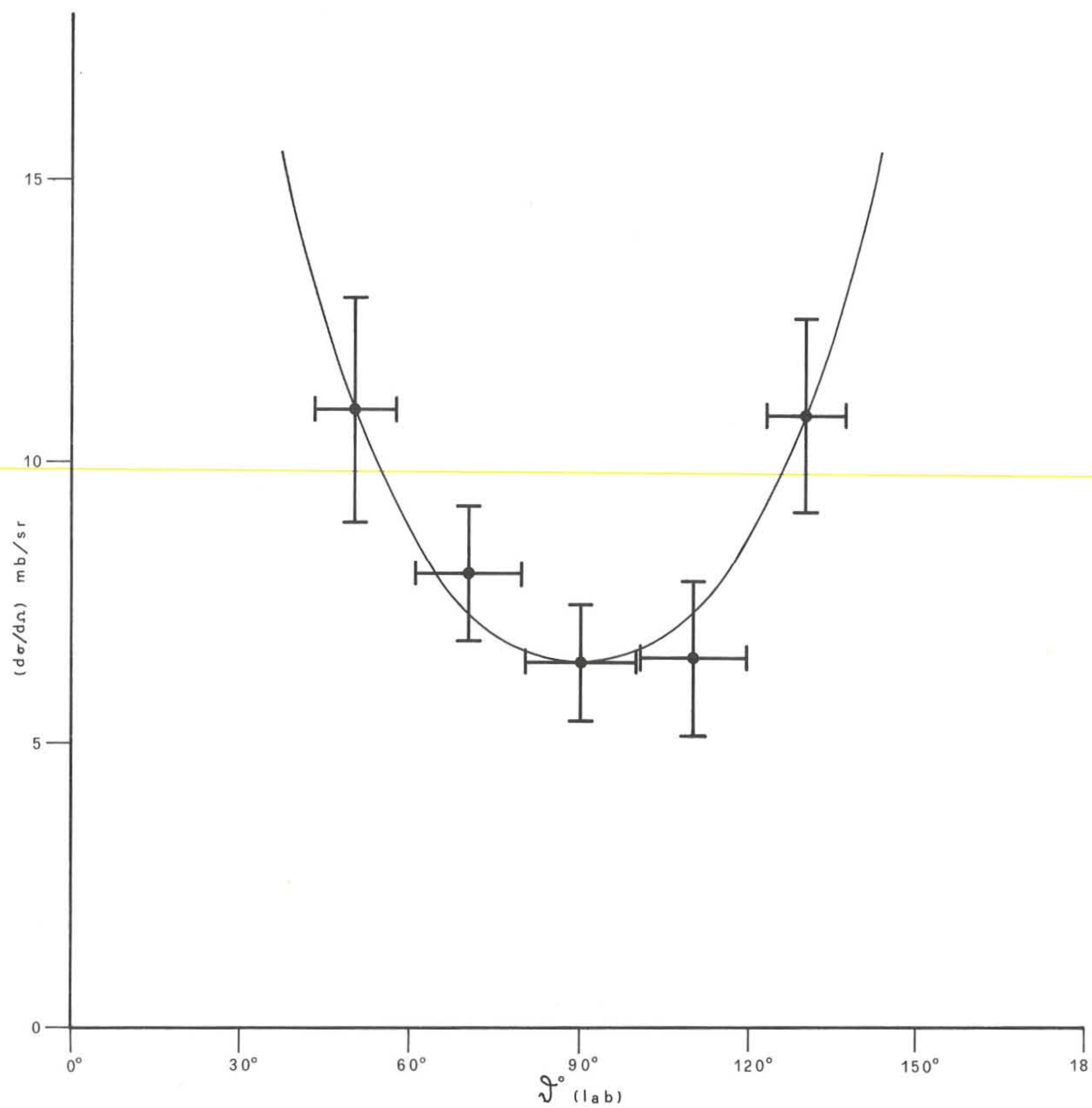

Fig. 10